Journal of Fluorine Chemistry 130 (2009) 799–805

Contents lists available at ScienceDirect

Journal of Fluorine Chemistry

journal homepage: www.elsevier.com/locate/fluor

Fluorination of alumino-silicate minerals: The example of lepidolite

Larisa P. Demyanova [a], Alain Tressaud [b,*]

[a] Institute of Geology and Nature Management, Amur Science Centre, Far Eastern Branch, RAS, Blagoveshchensk, Russia
[b] Institute of Condensed Matter Chemistry of Bordeaux (ICMCB-CNRS), University Bordeaux, 33608 Pessac, France

ARTICLE INFO

Article history:
Received 2 April 2009
Received in revised form 5 June 2009
Accepted 11 June 2009
Available online 24 June 2009
This paper is dedicated to Henry Selig in recognition to his great achievements in many fields of fluorine chemistry.

Keywords:
Fluorine
Rf-plasma
Fluorinated gases
Silicate
Mica
XPS
Surface modifications

ABSTRACT

The effect of fluorination on silicate and alumino-silicate minerals has been investigated, in particular on the lepidolite $[K(Li,Al)_3\ [Si_3AlO_{10}]\ (F,OH)_2]$ of the mica-type. The fluorination techniques included direct F_2-gas and cold radio-frequency-plasma involving c-C_4F_8 or O_2/CF_4 mixtures. The modifications of the surface properties have been followed mostly by XPS. Depending of the fluorination route used, either a reactive etching process involving M–F bonding occurs (direct F_2-gas; O_2–CF_4 rf-plasma), or a carbon fluoride deposition takes place (c-C_4F_8 rf-plasma).

1. Introduction

Silica and silicon-based oxides are major components of the earth's crust. These materials have attracted the attention of researchers because of applications in numerous fields. The properties of silica, silicates and alumino-silicates largely depend on the chemistry of their surface. Among the possible species that can help modify the surface properties of materials, the F^- ions, generating ionic bonds, have been largely used, in particular for silica [1–6]. Recently, the properties of amorphous silica generated by the fluoride method have been investigated [7–11]. This synthesis route has been extended to other types of silica and alumino-silicate deposits according to a close technological scheme providing total ecological security of industrial production [12]. On the other hand, the deposition of fluorocarbon films onto materials enables their uses in numerous electrical, mechanical, and biomedical applications due to adapted physicochemical properties of the film, including surface energy, friction, hydrophobicity and hemocompatibility.

The effect of fluorination on silicate and alumino-silicate minerals, in particular on phyllosilicates of the mica-type has been investigated in this work. The purpose is to functionalize the surface of these materials, either by a reactive etching process involving fluoride species or by a fluorocarbon film deposition. These materials are important from an applied point of view because of the combination of their physical, chemical and thermal properties: low power loss factor, dielectric constant and dielectric strength, account for their exceptional industrial interests. As far as the surface properties are concerned, X-ray photoelectron spectroscopy (XPS or ESCA) is a technique particularly suitable to study changes in binding energies (BE) of the different elements that are present within the utmost surface of the material [13,14]. After a general overview of possible fluorine substitutions in phyllosilicates, the attention will more particularly be focused on the lepidolite mineral of the mica-type, with $K(Li,Al)_3\ [Si_3AlO_{10}]\ (F,OH)_2$ composition [15].

2. Experimental procedure

2.1. The alumino-silicate samples

The studied alumino-silicate minerals came from Amur region deposits, Siberia and were characterized and analyzed at Blagoveshchensk Institute of Geology and Nature Management (FEB RAS). Lepidolite and muscovite were more particularly investigated since they were obtained as large flakes that could be cleaved into very thin, flexible, transparent layers. The surface of the flakes is perpendicular to *c* direction, as clearly shown by X-ray

* Corresponding author.
E-mail address: tressaud@icmcb-bordeaux.cnrs.fr (A. Tressaud).

0022-1139/$ – see front matter © 2009 Elsevier B.V. All rights reserved.
doi:10.1016/j.jfluchem.2009.06.009

Table 1
Compositional ranges of elements present in lepidolite mineral.

K_2O	4.82–13.85%	SiO_2	46.9–60.06%
Li_2O	1.23–5.90%	H_2O	0.65–3.15%
Al_2O_3	11.33–28.80%	F	1.36–8.71%

diffraction patterns. It should be noted that these flakes could be ground as powders. However in this case a structural disordering of the materials could occur, leading to an amorphization, as shown by the X-ray diffractograms. A set of analytical characterizations was used, i.e. X-ray diffraction, X-ray fluorescence, microprobe, and IR spectroscopy. X-ray diffraction and fluorescence analyses were carried out on a DRON-3M device and a BRUKER S4 PIONEER spectrometer, respectively. The morphology of samples was studied using a LEO-1420 high-resolution focused beam microscope with 12–257,000 extension range. The obtained samples were identified by IR spectroscopy on a Spectrum-One IR Fourier spectrophotometer PerkinElmer-2002, which allows characterizing the types of hydroxyl groups.

Because of numerous possible substitutions that may occur within the two-dimensional structures of alumino-silicate minerals, the compositional range appears to be rather wide. In the case of the lepidolite sample with mica-type coming from deposits of the Amur region, the oxide analysis is comprised within the limits given in Table 1.

An example of the overview XPS spectra is given in the case of as-received lepidolite flakes, cleaved before their introduction in the vacuum chamber (Fig. 1a). The Si/Al atomic ratio is of 3/1.8 and the presence of excess oxygen and carbon, even in cleaved sample, might be due to the presence of some surface carbonation. C1s + K2p, F1s, Al2p and Si2p spectra of as-received lepidolite crystals are given in Fig. 2. Fluorine is present in noticeable amounts in the sample (~1 to 4 wt.%), whereas in the case of muscovite sample the amount is significantly lower (0.5 wt.%). F1s FWHM is equal to 2 eV and the envelope is centred at BE = 685.4 eV, in good agreement with F–Al bonding. F1s peak can be best fitted into several components that account for the presence in the network of different cationic environments around fluorine atoms (Li, Al, Si, K). The C1s contribution is mostly due to contamination carbon. It can be pointed out that the presence of K2p doublet renders more difficult the fitting of the high BE part of C1s spectrum once the material is fluorinated. FWHM of Al2p and

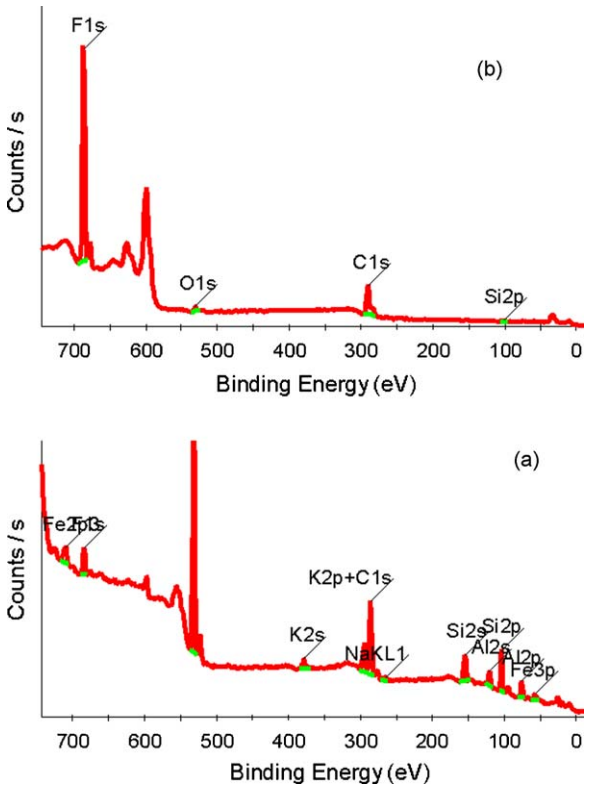

Fig. 1. Overview XPS spectra of lepidolite crystal flakes from Amur region, Siberia: (a) as-received and (b) rf-plasma treated with c-C_4F_8.

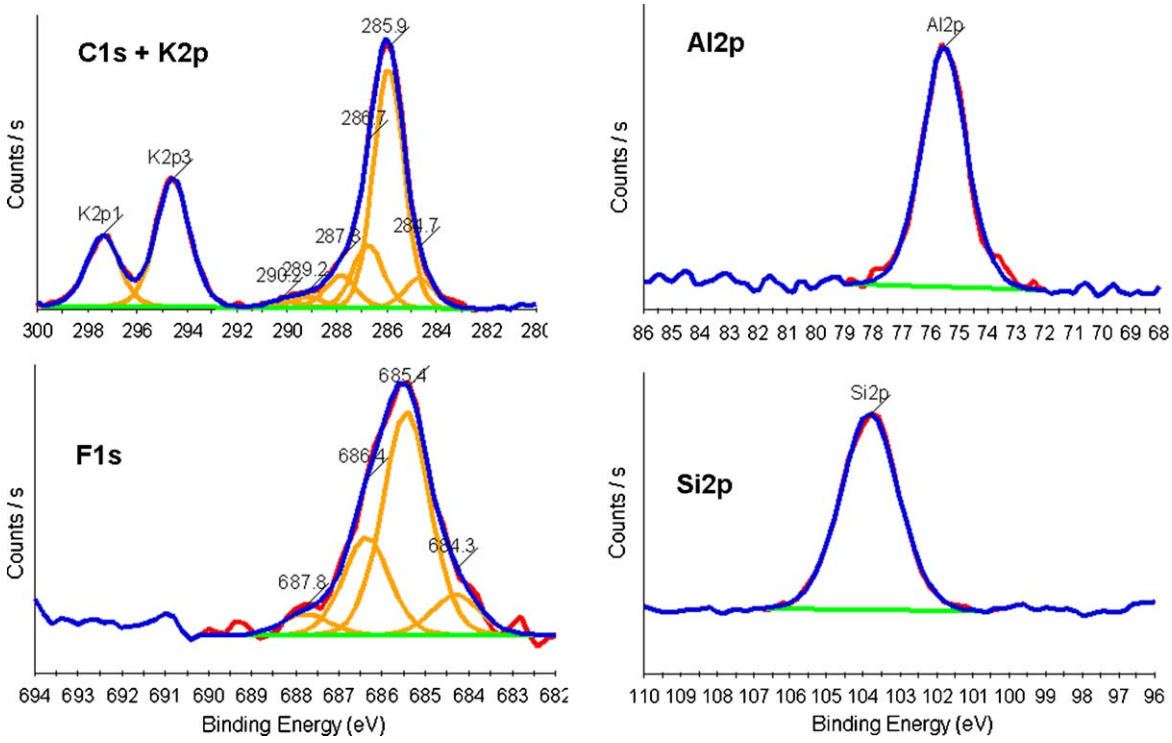

Fig. 2. C1s + K2p, F1s, Al2p and Si2p XPS spectra of as-received lepidolite flakes.

Si2p envelopes are equal to 2.1 and 2.2 eV, respectively, allowing to fit the envelope with only one type of Al–O and Si–O bonding. In these insulating materials a significant charge effect may occur, depending on the difference in conductivity of the different domains. This effect may lead to a shift in BE positions caused by differences in conductivity within the analyzed area (as illustrated in Fig. 4, in the low BE part of C1s spectrum).

2.2. Fluorination methods

2.2.1. Direct F_2-gas fluorination

Direct F_2-gas fluorination process was performed at various temperatures, between 100 and 200 °C in a "fluorine line" using handling procedures previously described, with adapted experimental set-up enabling to work in excellent safety conditions [5]. The samples were set in a Ni boat which had been previously passivated. F_2-gas, generally 10% diluted in N_2 (Air Products) was used at room pressure. The reaction duration depended on the starting materials but in most cases did not exceed 60 min, in order to limit the fluorination to the surface only. At the end of the experiment, F_2-gas was eliminated from the reactor and substituted by N_2.

2.2.2. Cold rf-plasma fluorination

Radio-frequency (rf) plasma fluorination is a low-temperature process where fluorinated gases are excited by an rf source and dissociated into chemically active atoms, radicals and molecules. Among the possible fluorinated gases, two were selected: CF_4 (tetrafluoromethane) and c-C_4F_8 (octafluorocyclobutane) which were excited by a rf source at 13.56 MHz. A primary vacuum was obtained by a 40 $m^3\ h^{-1}$ pump equipped with a liquid nitrogen condenser, which trapped the residual gases. The reactor comprised two cylindrical barrel-type aluminium electrodes which were coated with alumina and which were located within a distance of 2 cm from each other and several gas inlets allowing the use of gas mixtures. The inner electrode was connected to the rf source, the outer electrode was grounded. The sample to be treated was placed at the centre of the chamber, onto the inner electrode. The gas was introduced in the inner part of the reactor and then dissociated by electron impacts occurring between the two electrodes. Neutral species and radicals diffused from this plasma zone to the centre of the reactor where they reacted with the sample. The samples were generally pre-treated with an O_2 plasma before the plasma fluorination process, in order to render their surface more reactive. This pre-treatment removed adsorbed airborne organic pollution and filled oxygen vacancies at the surface of the sample.

In order to have a higher amount of $F^\bullet$ radicals, oxyfluorinated plasmas containing mixtures of O_2 (25%) and CF_4 (75%) were used. Reactions in O_2/CF_4 plasmas have been extensively studied by several authors [16,17]. Oxygen atoms produced in the discharge react rapidly with the CF_x radicals by free radical exchange. The products of reaction are atomic fluorine and relatively stable species (CO, COF or COF_2). The final reaction scheme corresponds to larger amount of fluorine and stable molecules (CO_2). The main effect upon addition of oxygen to CF_4 is thus a strong increase in the concentration of fluorine in the gas phase, and a drastic decrease in the CF_x radicals density, as confirmed by optical diagnostics [18]. The interest for surface fluorination is obvious since it allows to increase the net fluorine flux onto the surface and prevents the formation of fluorocarbon films [19].

Under rf-plasma conditions, c-C_4F_8 molecules behave a totally different process. They dissociate into neutral radicals (e.g., CF, CF_2, CF_3), ions ($C_2F_4^+$), and stable molecules (e.g., C_2F_4, some non-dissociated C_4F_8 [20]). It has been shown that CF_2 species are the dominant CF_x radicals [20] which further deposit onto the treated material, forming a fluorinated layer of average CF_2 composition. Recent studies dealing with octafluorocyclobutane rf-plasmas have confirmed that the film growth is controlled by C_xF_y ions and neutrals. The efficiency of the film deposition was investigated in terms of size of the monomer precursors, in particular $C_2F_4^+$ ion species [21,22]. In the case of SiO_2 substrates, the adhesion of the film can be drastically improved by inserting an adhesion promoter consisting of Si-rich SiO_2 [23]. However in our case the adhesion level could not be evaluated by peeling experiments for instance.

Parameters that may be varied during the plasma fluorination process are pressure and flow of the gases, temperature and reaction duration [24]. All plasma processes were carried out with an rf power of 80 W. The pressure of the gas in the reactor could be varied between 10 and 300 mTorr, the temperature was thermostatically controlled and maintained between room temperature and 90 °C, whereas the duration of the treatment could take from a few minutes up to one hour. The conditions generally used in the following were: p = 100 mTorr, P = 80 W, t = 60 min, T = 25 °C.

2.3. Surface analyses

XPS analyses were performed with a VG 220 i-XL ESCALAB. The radiation was an Mg non-monochromatized source (1253.6 eV) at 100 W. 150 μm diameter areas were investigated on each sample. The insulating character of the silicate samples needed low-energy (4–6 eV) electron compensation. Survey and high-resolution spectra were recorded with pass energy of 150 and 20 eV, respectively. When fitting the C1s envelopes, each component was considered as having similar FWHM, i.e. 1.5 eV. This procedure appeared to be the most reliable one, as previously proposed in investigations on fluorinated carbon materials [25]. A good agreement between the experimental curve and the full-calculated envelope was obtained, which allowed explaining in addition subtle distinctions between the proportions of fluorinated carbon components. As these materials are non-conductive, flood gun has been activated onto the samples to shift the high-resolution spectra in their normal range (i.e. 285–293 eV for C1s). Quantification of F, Si, Al, O, and C elements was obtained with an Advantage processing program provided by Thermo Fisher Scientific. The BE values were generally determined with respect to the Si2p BE in silica and silicates: BE = 103.5 eV.

3. Results and discussion

3.1. Fluorine substitution in alumino-silicates

It is well known that numerous substitutions may occur in silicate and alumino-silicate minerals, either in the cationic network or in the anionic one. In the latter one, oxygen may be substituted by other anionic species, in particular by hydroxyl or fluoride groups. Among the various classes of silicates, the phyllosilicate group is of particular interest because the network offers numerous possibilities of cationic or anionic (O^{2-}, OH^-, F^-) substitutions and/or intercalations.

In numerous types: pyrophyllite, talc, mica (muscovite, lepidolite), clays (montmorillonite) or chlorite the basal layer structure is based on t-o-t arrangements between SiO_4 tetrahedra and MO_6 octahedra (also called 1:1 layers). Numerous polytypes exist in the mica group of general formula $^{xii}A^{vi}R_{2-3}{}^{iv}T_4O_{10}(OH,F)_2$ (with T = Si, Al), A being generally a monovalent (alkaline) or a divalent (alkaline-earth) cation, R being not only a trivalent (Al^{3+}) but also possibly a monovalent or divalent cation. The minerals of the mica group include: muscovite: $KAl_2[Si_3AlO_{10}](F,OH)_2$; lepidolite: $K(Li,Al)_3\ [Si_3AlO_{10}]\ (F,OH)_2$; biotite: $K(Fe^{2+},Mg)_3[Si_3AlO_{10}]\ (F,OH)_2$. The periodicity of t-o-t stacking is about 10 Å or a multiple

value, and depending on the rotation angle between successive shifts, different polytypes can be found. Whereas muscovite is the prototype of dioctahedral micas $^{xii}A^{vi}R_2{}^{iv}T_4O_{10}(OH,F)_2$ with mostly the 2M1 polytype ($C2/c$ space group), lepidolite is one of trioctahedral micas (phlogopite-type) $^{xii}A^{vi}R_3{}^{iv}T_4O_{10}(OH,F)_2$ with possible 1M and 2M2 polytypes ($C2/m$ or Cm, and $C2/c$ space groups, respectively). As an example, the XRD pattern of the studied lepidolite crystal is given in Fig. 3. Main peaks correspond to 0 0 l indices. The diffraction peaks can be indexed in the 1M polytype with $C2/m$ monoclinic symmetry and unit cell constants: a = 5.242 Å, b = 9.055 Å, c = 10.09 Å, β = 100.77° (cf. ICDD no. 85-0912) [25]. It should be noted that some $k\,h\,l$ indices exhibit somewhat different intensities with respect to the ICDD file, because of slightly different elemental composition.

3.2. Fluorination treatments of alumino-silicate minerals: the example of lepidolite

3.2.1. Deposition of a carbon fluoride layer by c-C_4F_8 rf-plasma treatment

The rf-plasma treatments have been carried out at room temperature, in the above detailed conditions. The formation of a carbon fluoride coating by c-C_4F_8 rf-plasma treatments on mica-type minerals can be illustrated by XPS results obtained on lepidolite flakes (Figs. 1b and 4). It is well known that the C1s envelope may spread over 10 eV because of the strong electro-negativity of fluorine. In addition to contamination, sp^3C or sp^2C, most contributions that appear at higher BE can be attributed to C–F_n bonds. The positions of these various C1s components have been determined using a previously proposed procedure, with respect to saturated non-functionalized sp^3C, whose BE after charging-effect correction is set in the 284.5 eV range [26]. Above BE = 287.0 eV, the components can be assigned to C atoms that are directly bound to F atoms, the BE increasing with increasing number of neighboring fluorine atoms. In between 285 and 287 eV, the components correspond to C atoms that are not directly bound to F atoms. In this range, the BE shift is due to an inductive effect which is again dependent on the number of F atoms in β position of a given C atom, that are bound to his first C neighbor. The shift can be evaluated to about 0.6 ± 0.2 eV for each F atom and is approximately additive. The proposed assignment is given in Table 2. In the survey spectra of C_4F_8-treated materials, Al and other cations present in the pristine substrate can be hardly detected, which means that the coverage of the surface by the carbon fluoride layer has been fully achieved, as shown on the overview spectrum of lepidolite (Fig. 1b). Only very small amounts of Al, Si, O could be detected at the surface. The surface composition is given in Table 3. After an etching using an Ar beam, the thickness of the CF_n ($1 < n < 3$) layer has been evaluated to be around 50 nm. In the C1s spectrum (Fig. 4) the most important contribution is detected at around 292 eV and corresponds to CF_2 species, with a shoulder at higher BE (CF_3 groups at BE = 293.8 eV). Numerous weak contributions are also found at lower BEs, which account for carbons with less fluorinated environments. It should be noted that the behaviour is similar for both treated muscovite and lepidolite crystals. For both crystals, the F1s peak occurring around 688 eV is assessed to covalent F–C bonding, as found for instance in PTFE, fluorinated carbons or graphite fluorides with CF_2 composition [27]. However the envelope can be best fitted with two additional environments for fluoride atoms, illustrating the presence of CF_3 group at higher BEs and less fluorinated groups at lower BEs.

When samples of lepidolite or muscovite are ground, the core of the material is more accessible to fluorination reactions. Therefore, because of the highly divided surface, the c-C_4F_8 rf-plasma treatment gives rise to two types of contributions, as observed in the F1s spectrum. The main F1s contribution is centred around BE = 688 eV and corresponds to F–C bonding of the carbon fluoride

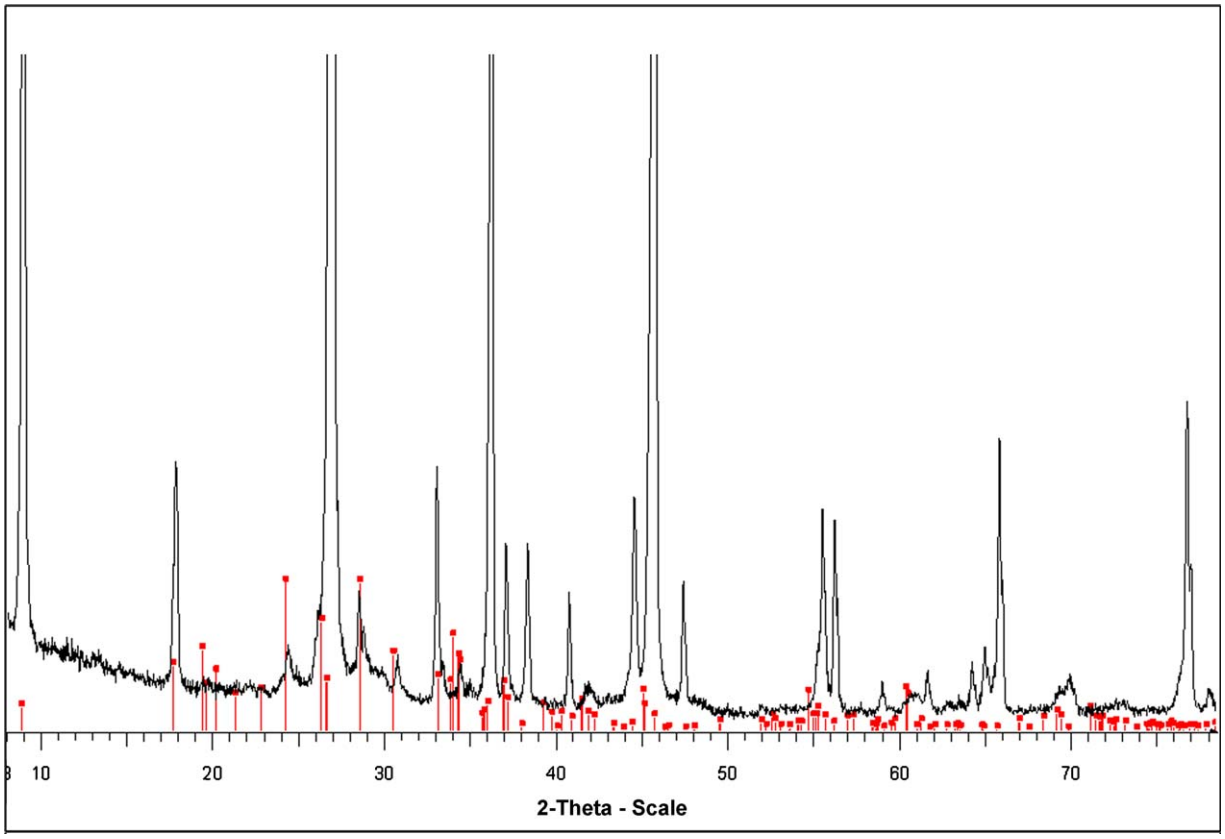

Fig. 3. X-ray diffraction pattern of lepidolite mineral from Amur region. The vertical bars correspond to the Bragg positions of ICDD no. 85-0912 (1M polytype).

Table 2
Assignment of C–F bonds in C1S XPS spectra of fluorinated carbon materials.

Involved bonds	sp^2C, sp^3C, contamination carbon	Non-fluorinated C in fluorinated environments (β position)	C–F in weakly (or non-) fluorinated environments	C–F in fluorinated environments	CF_2 in a weakly fluorinated environment	CF_2 in fluorinated environments (CF_2–CF_2 at 292 eV)	CF_3 and CF_2 in highly fluorinated environments
BE (eV)	284–285	285.5–287	287–288	288–289	290–291	291–292	293–294

Table 3
Surface composition (atomic%) of as-received and c-C_4F_8-treated muscovite and lepidolite flakes (source RX TWIN Mg, Ep = 20 eV, Scofield correction, relative error ± 5–10%).

Element	C	O	F	Si	Al	K	Other
Muscovite flake	9.9	56.6	0.5	14.8	12.4	4.4	Na: 1.4
Muscovite flake/rf-plasma c-C_4F_8	29.6	6.4	57.8	3.0	2.4	0.7	–
Lepidolite flake	25.0	43.8	3.9	13.8	7.9	3.5	Fe: 1.9
Lepidolite flake/rf-plasma c-C_4F_8	32.2	2.0	63.8	1.0	0.6	0.4	–

coating, whereas the contribution at lower binding energy: BE = 685 eV, is due to bonding between fluorine and metal (Al or K). Such a type of spectra is illustrated in Fig. 5 in the case of the lepidolite ground sample. The fluorination appears thus to be less homogeneous than in the case of flaky samples, with some parts of the surface fully covered by CF_n coating and other parts exhibiting surface Al–F (or K–F) bonds. However, the results on ground samples should be taken cautiously since an amorphization of the material is found, as quoted above, and may therefore change the nature of the general structure and environments in the materials.

3.2.2. Reactive etching of the surface by F_2-gas and O_2–CF_4-plasma treatments

In term of species that interact at the substrate surface, rf-plasma treatments using O_2/CF_4 mixtures have many common points with F_2-gas treatments. In both cases the fluorination take place trough $F^\bullet$ radicals or F_2 species. The major difference is of course that in the case of the plasma treatment the reaction is limited to 50–100 nm from the surface, whereas F_2 gas may react to the core of the material. For F_2-gas treatments, the reaction temperature should be limited ($100\,^\circ C < T < 200\,^\circ C$) in order to reduce the etching phenomenon which is often associated with the presence of silicon in the minerals. When the etching takes place, lower amounts of silicon are found at the surface because of the departure of volatile SiF_4; the amount of Al and K conversely increases. In most cases, only Al–F bonds are observed. These points are illustrated in Fig. 6A with lepidolite flakes fluorinated by F_2-gas. C1s spectrum arises from pollution carbon, no clear CF_n contribution being noticeable. The F1s peak can be fitted into two components at 685 and 686 eV both accounting for bonding between fluorine and cations present in the structure, such as Al, Li, K, Si. In the Al2p peak the major contribution, at BE = 76.5 eV, is 1 eV higher than the one in oxygenated surrounding and accounts

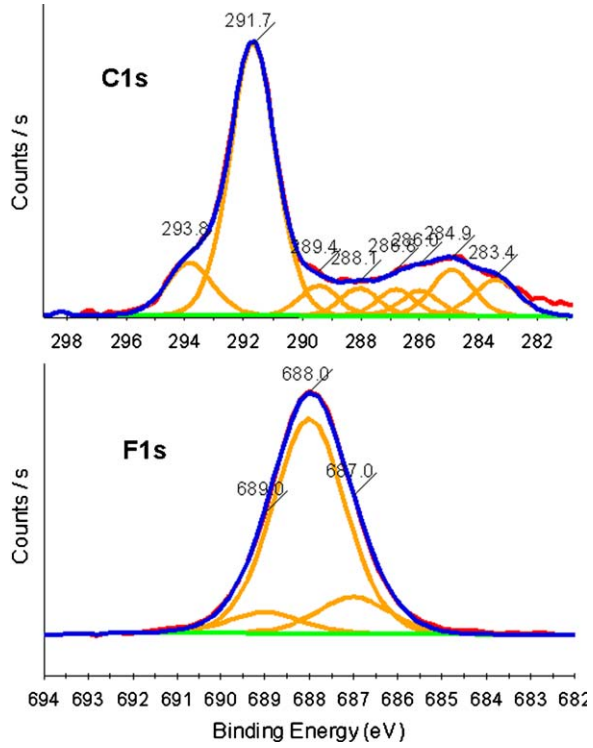

Fig. 4. Fitted C1s and F1s XPS spectra of c-C_4F_8 plasma-treated lepidolite flakes.

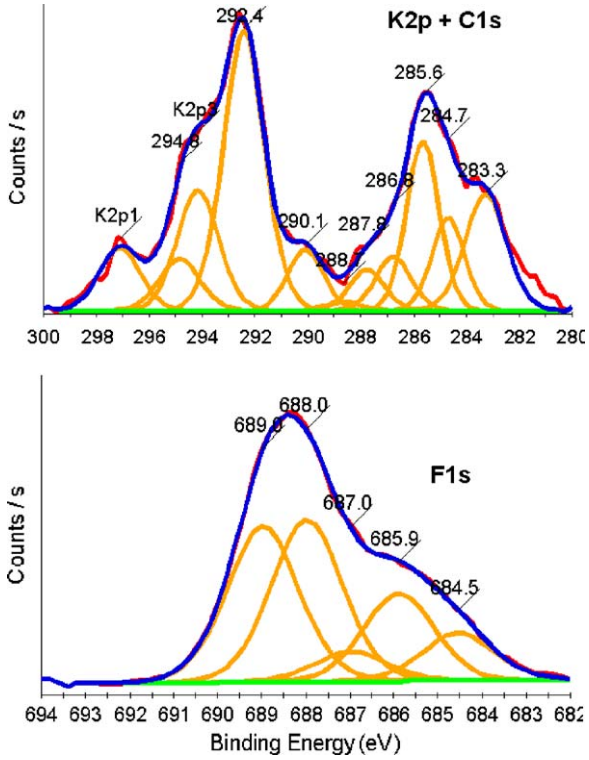

Fig. 5. C1s and F1s XPS spectra of c-C_4F_8 plasma-treated powdered lepidolite sample.

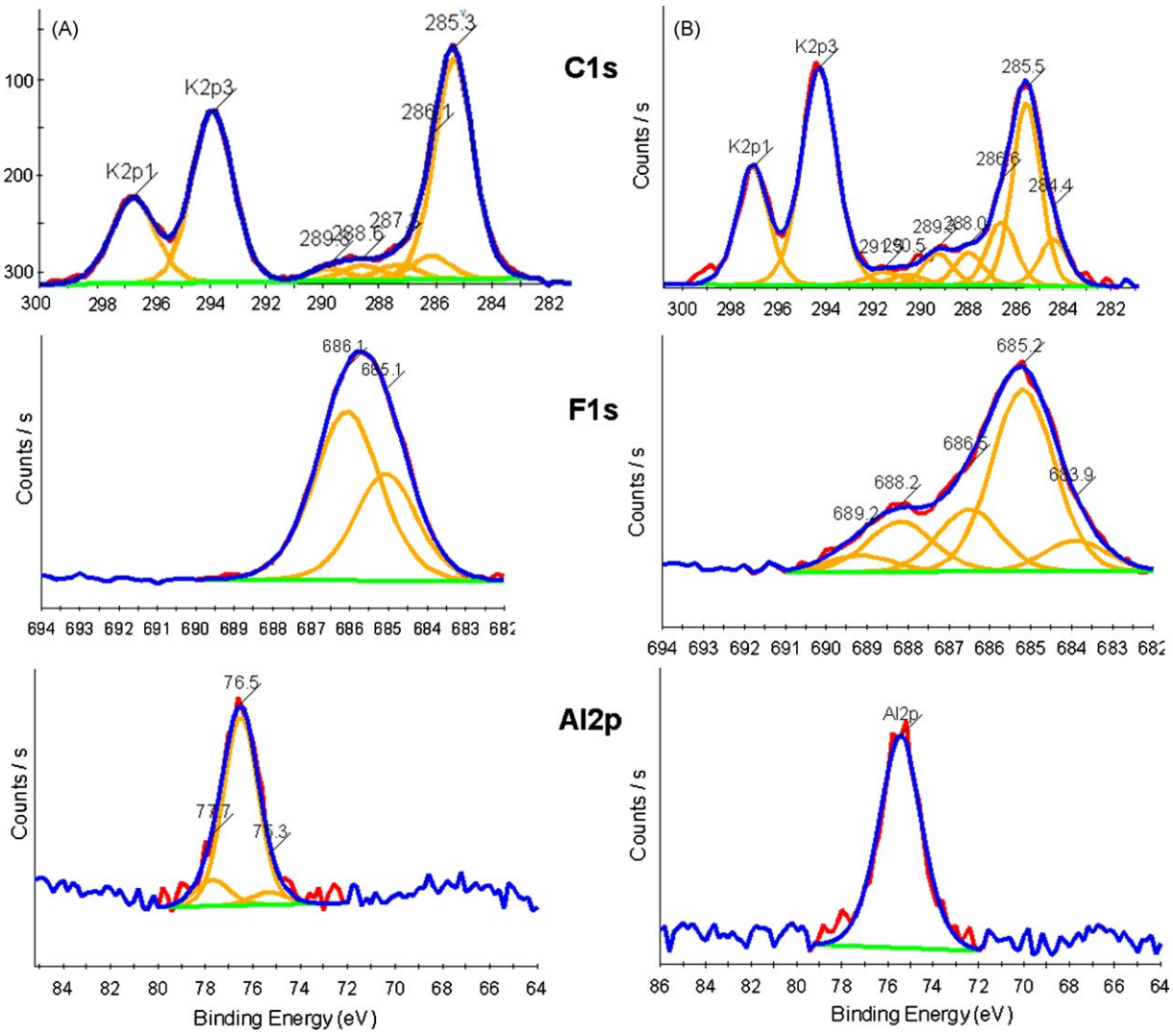

Fig. 6. Comparison of C1s, F1s and Al2p XPS spectra of F_2-gas treated lepidolite flakes (A), and O_2/CF_4 plasma-treated lepidolite flakes (B).

Table 4
Surface composition (atomic%) of rf-plasma and F_2-gas treated muscovite and lepidolite samples (source RX TWIN Mg, Ep = 20 eV, Scofield correction, ±5–10%).

Element	C	O	F	Si	Al	K	Other
Lepidolite powder/rf-plasma c-C_4F_8	27.7	14.4	46.8	6.1	3.4	1.6	–
Muscovite powder/rf-plasma c-C_4F_8	26.3	20.7	35.1	6.8	7.5	2.2	Na: 1.4
Lepidolite flake/rf-plasma O_2–CF_4	13.8	40.5	15.5	12.9	9.3	4.1	Fe: 3.9
Muscovite flake/rf-plasma O_2–CF_4	15.5	45.7	10.3	12.8	11.6	4.2	Na: limit
Lepidolite flake/F_2-gas	24.0	9.8	47.5	1.5	10.4	5.6	N: 1.0
Muscovite flake/F_2-gas	16.0	28.7	28.6	8.0	12.7	4.2	Na: 1.5, N: 0.4

for the highly fluorinated surface, that is 47.5% (Table 4). No CF_n is observed and the contributions present in the F1s spectrum, correspond to fluorine–metal bonding.

A comparison with O_2/CF_4 plasma-treatments is illustrated in Fig. 6A and B in the case of lepidolite crystals. The etching is less pronounced for plasma treatments, with larger amounts of silicon present at the surface (see Table 4). In oxyfluorinated rf-plasma conditions, some CF_n groups may be noticed in the C1s spectrum at higher BE (289–291.5 eV range), and the F1s envelope is much broader thus confirming the features of the C1s spectra. It should be added that in the case of ground samples, the fluorination by F_2-gas at 200 °C is so reactive that a decomposition of the materials occurs with about 30% weight loss, only 1.5% Si remaining on the surface (see Table 4). It is difficult to compare the spectra obtained in these conditions with the previous ones, because of this high weight loss.

4. Concluding remarks

It is known that the fluoride route is able to modify the networks of various microporous compounds: silica [5,6,11], zeolites and metallophosphates [28,29], clays [30,31], rending these phases attractive for numerous purposes, including catalysis [32]. The use of various fluorination techniques including rf-plasmas or direct F_2-gas extends this type of surface modifications, which can functionalize in a very versatile way various silicates of

the mica-type. Depending of the used fluorinating reagent, it is possible either to coat the flaky – or powdered – samples, with a protective layer of carbon fluoride, 50 nm thick, acting as a "teflonisation", or to create at the surface Al–F bonding. By these techniques some surface properties can be drastically modified, such as the hydrophilic/hydrophobic or the reactivity/passivity balances. It can be pointed out that the fluorocarbon coating process could allow these silicate minerals to be used in various applications because of the outstanding physicochemical properties of the film, including low surface energy, low friction coefficient, high hydrophobicity and high hemocompatibility. The investigation of the functionalization of silicates using fluorination routes will be extended in a forthcoming paper to several mica-type minerals.

Acknowledgements

Etienne Durand (ICMCB-CNRS) is acknowledged for fluorination treatments, Helene Serier for XRD files, and Christine Labrugère (CECAMA) for XPS experiments, spectra fitting and assignments.

References

[1] T. Katsuo, Y. Satohito, T. Kimio, Bull. Jpn. Pet. Inst. 12 (1970) 136.
[2] C.V.A. Duke, J.M. Miller, J.H. Clark, A.P. Kybett, Spectrochim. Acta, Part A 46 (1990) 1381.
[3] J.J. Pesek, M.T. Matyska, R.R. Abuelafiya, Chemically Modified Surfaces: Recent Developments, Royal Society of Chemistry, Cambridge, U.K., 1996.
[4] E.F. Voronin, A.A. Chuiko, Naykova Dymka, Kiev, 2001.
[5] E. Lataste, A. Demourgues, H. Leclerc, J.-M. Goupil, A. Vimont, E. Durand, C. Labrugère, H. Benalla, A. Tressaud, J. Phys. Chem. C 112 (2008) 10943–10951.
[6] E. Lataste, C. Legein, M. Body, J.Y. Buzaré, A. Tressaud, A. Demourgues, J. Phys. C, in press.
[7] L.A. Zemnukhova, V.I. Sergiyenko, V.S. Kagan, G.A. Fedorishcheva, Method of Generation of Amorphous Dioxide from Rice Peeling, Patent No. 2061656 Russia, MPK7 C 01 B 33/12, Application 1994.08.29, 1996 (Bulletin No. 16).
[8] T.S. Yusupov, et al., A Method of Generation of Amorphous Silica Dioxide, Patent No. 2261840 Russia, 2005 (Bulletin No. 28).
[9] D.S. Srebkov, V. Zadde, A. Pinov, et al. 11th Workshop on Crystalline Silicon Solar Cell Materials and Processes, Colorado, (2001), pp. 199–207.
[10] V.S. Rimkevich, Yu.N. Malovitski, L.P. Demyanova, Method of Processing of Silica Containing Material, Patent No. 2286947, Russia, MPK7 C01B 33/18, Application 2004.04.05, 2006 (Bulletin No. 31).
[11] L.P. Dem'janova, A. Tressaud, J.Y. Buzare, C. Martineau, C. Legein, Yu.N. Malovitsky, V.S. Rimkevich, Inorg. Mater. 45 (2009) 151–156.
[12] V.S. Rimkevich, Yu.N. Malovitskii, L.P. Demyanova, et al. Khim. Tekhnol. (no. 2) (2007) 65–71.
[13] D. Briggs, M.P. Seah, in: D. Briggs, M.P. Seah (Eds.), Practical Surface Analysis Auger and XPS, vol. 1, John Wiley, New York, 1990, and articles herein.
[14] A. Tressaud, E. Durand, C. Labrugère, J. Fluorine Chem. 125 (2004) 1639–1648.
[15] R.V. Gaines, et al. (Eds.), Dana's New Mineralogy, eighth edition, John Wiley & Sons, Inc., 1997.
[16] I.C. Plumb, K.R. Ryan, Plasma Chem. Plasma Process. 6 (1986) 205.
[17] J.C. Martz, D.W. Hess, W.E. Anderson, Plasma Chem. Plasma Process. 10 (1990) 261.
[18] A. Campo, Ch. Cardinaud, G. Turban, Plasma Sources Sci. Technol. 4 (1995) 398.
[19] C. Cardinaud, A. Tressaud, in: T. Nakajima, B. Zemva, A. Tressaud (Eds.), Advanced Inorganic Fluorides, Elsevier, 2000, p. 437 (Chapter 14).
[20] C.B. Labelle, R. Opila, A. Kornblit, J. Vac. Sci. Technol. A 23 (no. 1) (2005) 190–196.
[21] S. Tajima, K. Komvopoulos, J. Phys. Chem. C 111 (2007) 4358–4367.
[22] A. Kono, Y. Ohya, Jpn. J. Appl. Phys. 39 (2000) 1365–1368.
[23] T. Tatsumi, K. Endo, J. Photopolym. Sci. Technol. 12 (1999) 193–198.
[24] A. Tressaud, C. Labrugère, E. Durand, C. Brigouleix, H. Andriessen, Sci. China Ser. E Technol. Sci. 52 (2009) 104–110.
[25] S. Guggenheim, Am. Mineral. 66 (1981) 1221–1232.
[26] G. Nansé, E. Papirer, P. Fioux, F. Moguet, A. Tressaud, Carbon 35 (1997) 175–194, 371–388 and 515–528.
[27] N. Watanabe, T. Nakajima, H. Touhara, Graphite Fluorides, Elsevier, Amsterdam, 1988 T. Nakajima, N. Watanabe, Graphite Fluorides and Carbon–Fluorine Compounds, CRC Press, 1991
[28] P. Caullet, J.L. Paillaud, A. Simon-Masseron, M. Soulard, J. Patarin, C.R. Chim. 8 (2005) 245.
[29] J.L. Paillaud, P. Caullet, J. Brendlé, A. Simon-Masseron, J. Patarin, in: A. Tressaud (Ed.), Functionalized Inorganic Fluorides, Wiley-Blackwell, in press.
[30] A. Majid, S. Argue, D. Kingston, S. Lang, J. Fluor. Chem. 128 (2007) 1012–1018.
[31] R. Valsecchi, M. Viganò, M. Levi, S. Turri, J. Nanosci. Nanotechnol. 8 (2008) 1835–1841.
[32] E. Reale, A. Leyva, A. Corma, C. Martinez, H. Garcia, F. Rey, J. Mater. Chem. 15 (2005) 1742–1754.